REMARKS

Claims 1-40 are canceled. New claims 41-59 have been added. No new matter has been added. Accordingly, claims 41-59 are pending in the present application.

INTERVIEW SUMMARY

Applicants thank Examiner Yu for the courtesies extended during an in-person interview held on June 10, 2008. During the interview, applicants presented two articles discussing the novel method for immunogenic peptide identification useful for identify peptides useful in cancer vaccines. In particular, the Weinzierl et al. reference was discussed (Molecular & Cellular Proteomics, vol. 6, pp. 102-113) as well as Lemmel at al., Nature Biotechnology, Advanced Online Publication. These publications are attached hereto at Tab A. The claims were not discussed in detail, however applicants noted that a preliminary amendment would be filed to clarify the claims.

CONCLUSION

If a telephone interview would be of assistance in expediting prosecution of the subject application, Applicants invite the Examiner to telephone the undersigned at the number provided below.

The Commissioner is hereby authorized to charge any fees required for this filing to Womble Carlyle Sandridge & Rice, PPLC Deposit Account No. 09-0528.

Respectfully submitted,

WOMBLE CARLYLE SANDRIDGE & RICE, PPLC

Date: 7|14|08

Teresa A. Lavenue
Registration No. 47,737

Phone: (703) 394-2273
Fax: (703) 790-2623
P.O. Box 7037
Atlanta, GA 30357-0037
Customer No.: 26158

5

TAB A

Distorted Relation between mRNA Copy Number and Corresponding Major Histocompatibility Complex Ligand Density on the Cell Surface*⑤

Andreas O. Weinzierl‡, Claudia Lemmel‡, Oliver Schoor‡, Margret Müller‡, Tobias Krüger‡, Dorothee Wernet§, Jörg Hennenlotter¶, Arnulf Stenzl¶, Karin Klingel‖, Hans-Georg Rammensee‡, and Stefan Stevanović‡**‡‡

The major histocompatibility complex (MHC) presents peptides derived from degraded cellular proteins to T-cells and is thus crucial for triggering specific immune responses against viral infections or cancer. Up to now, there has been no evidence for a correlation between levels of mRNA (the "transcriptome") and the density of MHC-peptide complexes (the "MHC ligandome") on cells. Because strong dependences are of intrinsic importance for the detailed understanding of translation efficiency and protein turnover and thus for systems biology in general and for tumor immunotherapy in practical application, we quantitatively analyzed the levels of mRNA and corresponding MHC ligand densities in samples of renal cell carcinomas and their autologous normal kidney tissues. Relative quantification was carried out by gene chip analysis and by stable isotope peptide labeling, respectively. In comparing more than 270 pairs of gene expression and corresponding peptide presentation ratios, we demonstrate that there is no clear correlation ($r = 0.32$) between mRNA levels and corresponding MHC peptide levels in renal cell carcinoma. A significant number of peptides presented predominantly on tumor or normal tissue showed no or only minor changes in mRNA expression levels. In several cases, peptides could even be identified despite the virtual absence of the respective mRNA. Thus we conclude that a majority of epitopes from tumor-associated antigens will not be found in approaches based mainly on mRNA expression studies as mRNA expression reflects a distorted picture of the situation on the cell surface as visible for T-cells. *Molecular & Cellular Proteomics 6:102–113, 2007.*

Major histocompatibility complex (MHC)[1]-bound peptides reflect a snapshot of the dynamic protein pool (1) and can therefore provide insights into protein turnover and the transient cellular proteome (2–4). Class I MHC molecules present peptides (8–11 amino acids in length) (5) from degraded proteins on the cell surface to cytotoxic T-cells to allow the T-cells to discriminate between self and non-self (6). In addition to its original purpose, this detection system can be used for the selective removal of mutated cells displaying aberrant MHC-peptide complexes on their cell surface (7). Therefore the identification of disease-related MHC-peptide complexes is of utmost interest for immunodiagnostics and immunotherapy. Huge efforts are being undertaken to identify cancer-specific MHC-peptide complexes applicable for tumor immunotherapy (8–10). In this context, the identification of tumor-associated antigens (TAAs), which are predominantly expressed in tumor tissue, is one strategy being followed. Apart from differential comparisons of tumor and normal tissue proteomes (11), mRNA-based techniques are also being widely applied. DNA expression cloning, for example, has proved to be one successful method for the identification of TAAs (12), but it is being increasingly complemented by large scale gene expression analysis using DNA microarrays (13, 14). The generation of MHC-peptide complexes starts in the cytosol where proteins are degraded by the proteasome (15). The source proteins for proteasomal digestion range from long lived proteins over short lived proteins to defective ribosomal products (DRiPs) (16), which do not reach proper folding and functional state. DRiPs are thought to be responsible for more than 30% of all MHC-bound peptides (17). Irrespec-

[1] The abbreviations used are: MHC, major histocompatibility complex; ADFP, adipophilin; dNIC, differential N-terminal isotope coding; DRiP, defective ribosomal product; ERAAP, endoplasmic reticulum aminopeptidase associated with antigen processing; HLA, human leukocyte antigen; NHS, nicotinoyloxysuccinimide; RCC, renal cell carcinoma; TAA, tumor-associated antigen; TAP, transporter associated with antigen processing; ANXA4, annexin A4; CCNI, cyclin I; CD24, small cell lung carcinoma cluster 4 antigen; EHD2, EH-domain-containing protein 2; HMOX1, decycling heme oxygenase 1; PIGR, polymeric Ig receptor; PLXNB2, plexin B2; RBBP4, retinoblastoma-binding protein 4; TMED10, transmembrane trafficking protein 10; UGT1A6, UDP-glucuronosyltransferase 1 family, polypeptide A6; UMOD, uromodulin; ER, endoplasmic reticulum.

tive of their origin, a small part of peptides generated in the cytosol escapes further degradation and is transported via the transporter associated with antigen processing (TAP) into the endoplasmic reticulum (18) where they can be further trimmed N-terminally by proteases such as the endoplasmic reticulum aminopeptidase associated with antigen processing (ERAAP) (19). Finally, the peptides are loaded onto MHC molecules with the help of several proteins, which include tapasin, calnexin, and calreticulin, and are exported as MHC-peptide complexes onto the cell surface. An alteration that is thought to be crucial for the repertoire of MHC ligands is the induction of immunoproteasomal subunits by interferon γ for example. Upon interferon γ stimulation cells exchange the three proteolytic subunits of the proteasome (PSMB1, -2, and -5) with subunits of different proteolytic activity (LMP2, LMP7, and MECL1), a hallmark for converting normal proteasomes into immunoproteasomes (20, 21).

The entire MHC pathway has been investigated in depth often with a focus on the therapeutic potential. MHC-bound peptides can be used for stimulation and activation of cytotoxic T-cells that, for example, have been used successfully for the treatment of melanoma (22, 23). The identification of suitable T-cell epitopes is one of the bottlenecks in the large scale use of this tumor immunological strategy. Utilizable T-cell epitopes have to be both tumor-associated and match the patient's MHC repertoire. Several T-cell epitopes for T-cell-based tumor immunotherapy have already been described, but the identification is laborious, and not all *in vitro* defined T-cell epitopes are potent for triggering an immune response also *in vivo*.

Gene chip analysis is frequently used for the identification of TAAs (24, 25), but it has not yet been investigated whether an overexpression of mRNA also results in an MHC overpresentation of peptides derived from the respective protein. Thus, in this study MHC peptide presentation levels were compared with their corresponding transcription levels. We analyzed human clear cell renal cell carcinoma and autologous normal tissue in a combined transcriptome and human leukocyte antigen (HLA) ligandome approach. HLA:peptide levels were quantified by mass spectrometry using stable isotope labels, and mRNA levels were determined by gene chip analysis using DNA microarrays.

EXPERIMENTAL PROCEDURES

Materials—The HPLC reagents, trifluoroacetic acid, acetonitrile, formic acid, and HPLC water, were purchased from Merck. Peptide modification reagent O-methylisourea hemisulfate was purchased from Acros Organics. 1-([$^1H_4/^2D_4$] Nicotinoyloxy)succinimide (light or heavy dNIC-NHS; D represents deuterium) was synthesized as described elsewhere (26).

Elution of HLA-presented Peptides—HLA-presented peptides were obtained by immune precipitation of HLA molecules from solid tissues using a slightly modified protocol (27) that involves the HLA-A-, -B-, and -C-specific antibody W6/32 coupled to protein A-Sepharose or CNBr-activated Sepharose (Roche Applied Science) followed by acid elution and subsequent ultrafiltration.
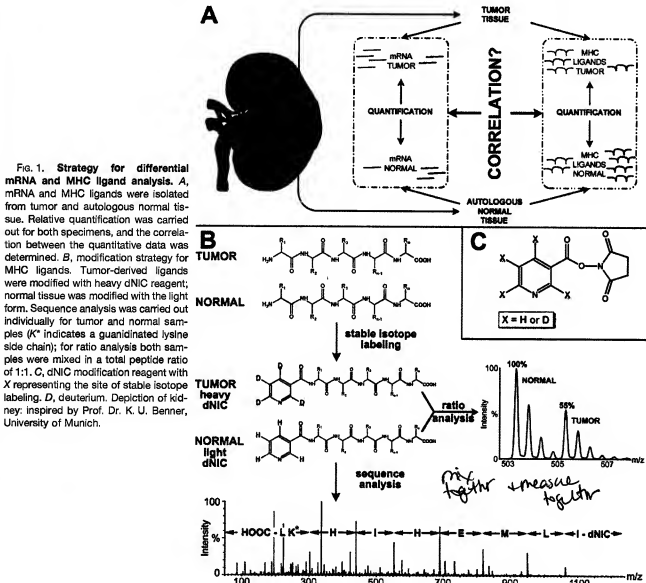
Modification of Peptides—Modification of peptides was carried out as described elsewhere (26) with slight modifications. In brief, peptide solutions were adjusted to pH 11 using 10 M NaOH and guanidinated at 65 °C for 10 min using 2.5 M O-methylisourea hemisulfate solution.

The reaction was halted by adjusting the pH to 3, and peptides were desalted by using Peptide Cleanup C$_{18}$ Spin Tubes (Agilent) as described in the manual. Peptides were loaded three times in 200-μl aliquots onto the Spin Tube columns. These were then washed three times with H$_2$O, and the peptides were nicotinylated on column for 15 min at room temperature. 500 μl of a 20 mM light or heavy dNIC-NHS solution in 50 mM phosphate buffer, pH = 8.5, were thus passed over the C$_{18}$ material with a flow rate of 35 μl/min. After washing the columns as described above, aminolysis of unwanted Tyr-dNIC esters was carried out by treatment with 500 μl of 50% hydroxylamine for 10 min at room temperature with a flow rate of 50 μl/min. Subsequently the columns were washed again, and the peptides were eluted using 4 × 50 μl of 60% acetonitrile, 1% formic acid.

Mixing of Peptides—To mix tumor and normal MHC peptides in a total peptide ratio of 1:1, absorption of isotope-labeled peptide pools was determined at 260 nm (28). Peptide content of the tumor and normal sample was calculated using the molar extinction coefficient for nicotinic acid in 50% acetonitrile ([cepsilon] = 1430 M^{-1}), and equal amounts of peptides were mixed.

Microcapillary LCMS—Peptide analysis was carried out as described elsewhere (26) using an Ultimate HPLC system (Dionex) with a gradient ranging from 15 to 55% solvent B within 170 min. Mixed tumor and normal samples were recorded in an LCMS experiment without fragmentation using a hybrid quadrupole orthogonal acceleration time of flight MS/MS system (Q-TOF, Micromass) equipped with a micro-ESI source. For sequence analysis tumor and normal samples were analyzed separately in individual LCMS/MS experiments.

Peptide Sequence Analysis and Peptide Quantification—Peptide sequence analysis was carried out manually. Therefore MS/MS spectra were smoothed using MassLynx 4.0 software (Savitzky-Golay, three smooth windows, two smooths). For manual peptide identification, sequence tag searches were done using Mascot 2.0 software (peptide and MS/MS tolerance, 0.2 Da; National Center for Biotechnology Information non-redundant (NCBInr) database updated monthly and restricted for search to human entries; 138,263 entries for human proteins at the time when the searches were done), and relevant hits were assessed manually and not by evaluation of the Mascot score. Criteria for manual identification were: a reasonable interpretation of at least 95% of all fragment peaks, complete sequence coverage with MS/MS fragments, and signal intensities of fragment ion peaks that match breakage probabilities of the respective sequence. For more than 50% of all sequenced peptides MS/MS spectra with both light and heavy dNIC isotope label were available, facilitating manual sequencing of the peptides. Ions containing the N terminus showed a mass shift of 4 Da due to the dNIC isotope label (see Fig. 2, C and D). In total 363 peptides were sequenced in the three analyzed RCC samples. All identified peptides were blasted against the NCBInr database (see above), and all peptides that could not be unambiguously allocated to only one protein sequence were excluded from further analysis unless the mRNA expression ratios for these potential source proteins were equal. All peptides that could be linked to an mRNA expression ratio Supplemental Table 1 lists protein information, HLA presentation ratio, mRNA expression ratio, HLA restriction, source, precursor mass, and charge state. All relevant MS/MS spectra used for peptide identification are available upon request. For peptide quantification mixed tumor and normal tissue samples were analyzed in an MS experiment. Peptide pairs were identified manually. Afterward mass chromatograms for the light and heavy versions of the peptide were calculated, and scans containing the peptide of interest were summed up. For background subtraction an equal number of scans with a similar retention time was subtracted. The relative amount of light and heavy dNIC peptides was calculated using the peak heights of the first isotope peaks (see Fig. 2B).

Fig. 1. **Strategy for differential mRNA and MHC ligand analysis.** *A*, mRNA and MHC ligands were isolated from tumor and autologous normal tissue. Relative quantification was carried out for both specimens, and the correlation between the quantitative data was determined. *B*, modification strategy for MHC ligands. Tumor-derived ligands were modified with heavy dNIC reagent; normal tissue was modified with the light form. Sequence analysis was carried out individually for tumor and normal samples (*K** indicates a guanidinated lysine side chain); for ratio analysis both samples were mixed in a total peptide ratio of 1:1. *C*, dNIC modification reagent with *X* representing the site of stable isotope labeling. *D*, deuterium. Depiction of kidney: inspired by Prof. Dr. K. U. Benner, University of Munich.

Assessment of False Positive Rate of Peptide Identification—To estimate the false positive rate of the identified peptides, a database was designed that contained both the European Bioinformatics Institute International Protein Index human database (IPI, version 3.21, containing 60,822 entries) and the reversed European Bioinformatics Institute International Protein Index human database (rIPI). 50 randomly chosen peptides from RCC099 were searched using the manually identified sequence tags in this database with the Mascot software. In summary 20% of all searches returned only one peptide with a significant Mascot score, and 66% of all searches returned only one hit (all in IPI). Only 6% of all searches resulted in more than three peptide hits (both in IPI and rIPI, Supplemental Table 2). Eight of theses peptides and eight additional peptides, also identified in RCC099, were chemically synthesized and modified (Supplemental Table 3). Fragmentation spectra of these synthetic peptides were compared with the fragmentation spectra recorded from RCC099. All synthetic peptides showed exactly the same fragmentation pattern as the peptides identified in RCC099. Thus we conclude that the false

positive rate in our sequence analysis is below 1%. Comparisons of MS/MS spectra obtained from synthetic peptides and from RCC099 are available upon request.

Gene Expression Analysis by High Density Oligonucleotide Microarrays—RNA isolation from tumor and autologous normal kidney specimens and gene expression analysis by Affymetrix Human Genome U133 Plus 2.0 oligonucleotide microarrays (Affymetrix, Santa Clara, CA) were performed as described previously (29). Data were analyzed with the GeneChip Operating Software (Affymetrix). Pairwise comparisons between tumor and autologous normal kidney were calculated using the respective normal array as base line.

RESULTS

Principles of Quantitative Peptide and mRNA Analysis—The general strategy used to assess the correlation between mRNA ratios and their corresponding ratios of HLA-presented peptides is depicted in Fig. 1*A*. mRNA was isolated from three
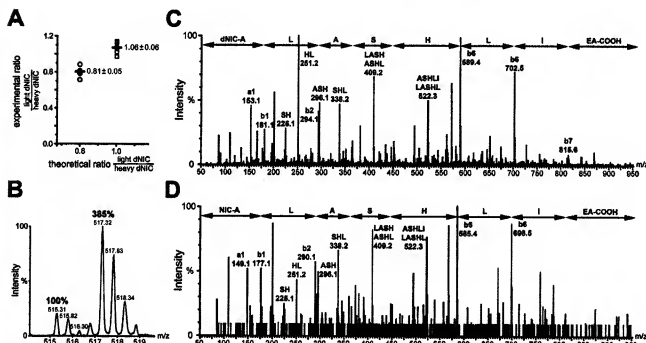
Fig. 2. Peptide ratio analysis and sequence identification. *A,* for estimation of methodical deviations a mixture of six synthetic peptides was modified with the dNIC strategy using either heavy or light dNIC in two independent experiments. Heavy and light samples were mixed in a total peptide ratio of 0.8:1 or 1:1. Actual peptide ratios were determined by mass spectrometry; mean and S.D. are stated. *B–D,* MHC ligands were isolated from RCC100 tumor and normal tissue and subsequently labeled differentially with heavy or light dNIC, respectively. Ratio determination of differentially labeled ALASHLIEA was done in MS mode (*B*). MS/MS fragment spectra (*C* and *D*) were used for sequence identification.

different RCC tumor tissues and respective autologous normal tissues for subsequent gene chip analysis. HLA-presented peptides were isolated from the same tumor and normal tissue samples (30) and quantified relatively as shown in Fig. 1*B* using the differential N-terminal isotope coding (dNIC) strategy (26, 28). The HLA ligandome isolated from tumor tissue was derivatized with "heavy" nicotinic acid (deuterium-bearing, Fig. 1*C*), whereas for the HLA ligandome of normal tissue the "light" nicotinic acid (hydrogen-bearing, Fig. 1*C*) was used. As a consequence, all peptides from tumor tissue possessed the very same physicochemical features as their counterparts with identical sequence from normal tissue but differed in mass by 4 Da. To achieve the highest possible accuracy and sensitivity both for quantification and sequence identification, quantification and sequence identification experiments were carried out separately. Therefore, after derivatization one aliquot of each peptide pool was used for relative quantification. Heavy dNIC-peptides from tumor samples and light dNIC-peptides from normal tissue were mixed in a total peptide ratio of 1:1 and subjected to on-line coupled ESI-LCMS. Pairs of identical peptides derived from tumor and normal tissue were identified on the basis of a 4-Da mass difference introduced by the isotope label and due to their identical retention times in chromatography. For differential quantification, the ratio of signal intensities between monoiso-

topic peaks of the tumor- and normal tissue-derived peptide was calculated (Fig. 1*B, right panel*). For peptide sequence analysis, the remaining aliquot of derivatized HLA ligand pools was used for peptide sequence analysis by on-line coupled ESI-LCMS/MS. Fragmentation experiments were carried out separately for each tumor and normal tissue (Fig. 1*B, bottom panel*). Thus an unambiguous allocation to tumor or normal tissue was possible for each peptide signal even in the case of peptides for which the corresponding sequence could not be determined. The separate analysis of tumor and normal tissue also allowed the exclusion of singlet signals, which occurred due to incomplete modification with dNIC, from further analysis. Quantitative information was linked to sequence information by peptide individual features combining mass, charge state, and retention time. To estimate the intrinsic methodological error, this quantification strategy was also applied to synthetic peptide pools, resulting in a calculated error for peptide pairs with high MS signal intensity of less than 10% (Fig. 2*A*).

mRNA Versus HLA Peptide: Quantitative Comparisons—In our study, this relative mRNA and HLA peptide quantification strategy was extended to three RCC samples sharing two HLA alleles: RCC099 (HLA-A*02, -A*03, -B*27, and -B*57), RCC100 (HLA-A*02, -A*03, -B*07, and -B*18), and RCC110 (HLA-A*02, -A*68, -B*18, and -B*27). Table I gives an over-

TABLE I
Absolute numbers of evaluated mRNA ratios, HLA ligand ratios, and peptide sequences identified in this study

In the last column for all RCCs the number of successful allocations of peptide sequences to the corresponding HLA ligand ratios and mRNA ratios is given.
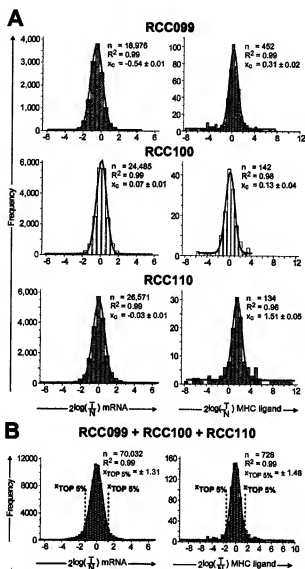
Source	mRNA ratios	HLA ligand ratios	Identified peptide sequences	Allocated sequence, peptide, and mRNA ratio
RCC099	18,976	452	213	166
RCC100	24,485	142	59	43
RCC110	26,571	134	91	64
Total	70,032	728	363	273

view of the identified mRNA and HLA peptide ratios, the number of identified sequences, and the peptides for which sequence information could be linked to its corresponding presentation ratios. In total, intensity ratios between tumor and normal tissue were determined for 728 peptide pairs (Fig. 2B), 363 peptides of which could be sequenced (Fig. 2, C and D). 273 peptide sequences could be linked to a specific mRNA ratio allowing the evaluation of a possible correlation between differences in gene expression and HLA peptide presentation (Supplemental Table 1).

To be able to combine the HLA-mRNA comparisons of all three RCCs datasets, relative mRNA expression ratios and HLA peptide presentation levels had to be evaluated individually for each analyzed tissue pair (Fig. 3A). To do so, histograms of logarithmized HLA peptide presentation levels were plotted and subsequently fitted assuming a Gaussian distribution. Each fitted HLA histogram plot had its maximum near 0, representing a 1:1 ratio of presentation on tumor and normal tissue. To take experimental inaccuracies into account regarding the mixing of HLA peptides from each tumor and normal tissue pair, the HLA presentation ratios were normalized such that the maxima of their fitted histogram plots were located at 0. Normalized HLA peptide presentation data of all three RCCs were cumulated and fitted assuming a Gaussian distribution to determine the presentation level representing the 5% highest over- or underrepresentation ($x_{TOP\ 5\%}$; Fig. 3B). An analogue normalization and assessment of the $x_{TOP\ 5\%}$ was carried out for the mRNA expression data.

Finally normalized mRNA ratios were plotted against their corresponding normalized HLA presentation ratio (Fig. 4), and the Spearman rank correlation coefficient was calculated at $r = 0.32$, showing an even weaker correlation of transcriptome to HLA ligandome than the correlation of transcriptome to proteome ($r = 0.45$) (4). For qualitative data analysis and simplified data discussion Fig. 4 was divided into nine areas by the $x_{TOP\ 5\%}$ margins of mRNA and peptide ratios as indicated by the *dashed lines* (Fig. 3B).

HLA Ligand Pools Derived from Tumor and Normal Tissue—For ~75% of all identified HLA ligands we could not detect significant changes either in their HLA presentation ratio or in

Fig. 3. **Normalization of quantitative mRNA and MHC ligand data.** mRNA ratios (*left panels*) and MHC ligand ratios (*right panels*) between tumor and normal tissue were logarithmized, and frequency counts were made with bin sizes from 0.3 to 0.7. The bin sizes were chosen so that the Gaussian fit resulted in the best R^2 values. Using these Gaussian fit functions, the mean value (x_c) of each data set was calculated. A shows data sorted for RCC099, RCC100, and RCC110. All data were normalized to $x_c = 0$. B, the margins of relative gene transcript expression representing the 5% strongest over/underexpression ($x_{TOP\ 5\%}$) were calculated as follows. Normalized mRNA data for all RCCs were cumulated and fitted assuming a Gaussian distribution, the area under this curve was calculated, and the *x* values corresponding to 5% (for underpresentation) and 95% (for overpresentation) of the area were determined. $x_{TOP\ 5\%}$ of the HLA ligandome ratios was calculated similarly. *T*, tumor; *N*, normal.

their corresponding mRNA expression levels (Fig. 4, *area V*). Regarding mRNA expression this might have been expected as it indicates on a transcriptional basis that the tumor tissue
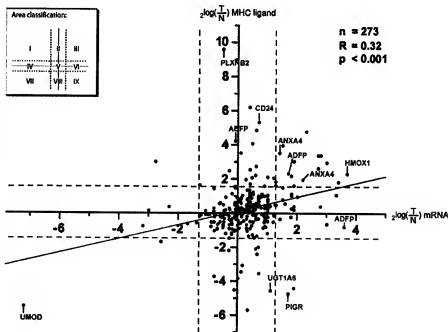
Fig. 4. **Scatter plot representation of the correlation between relative mRNA expression and relative MHC ligand presentation.** The $\log_2$ of the mRNA and MHC ligand ratios of tumor *versus* normal tissue were calculated and plotted for 273 pairs of mRNA and MHC ligand ratios. Linear regression is shown as a *solid line*, and the Spearman rank correlation coefficient was calculated. *Dashed lines* designate the margins for the 5% of mRNA ($x = \pm 1.3$) and peptide ($y = \pm 1.5$) specimens with the highest under- and overexpression, respectively, presentation. Thus, the plot is divided into nine areas (see inset). Selected loci are highlighted. *T*, tumor; *N*, normal.

still resembles its corresponding normal tissue. As to the HLA level this is more surprising as gene chip analysis showed up-regulation of interferon γ-inducible proteins in the antigen-processing machinery (Table II). In all tumor tissues analyzed, immunoproteasomal subunits were clearly overexpressed (up to 11-fold for LMP2 in RCC110). Although immunoproteasomal activity is thought to change the HLA-bound peptide repertoire (31) and although it has been shown that both normal and immunoproteasomes are capable of destroying each other's epitopes (32, 33), we could not detect major differences in the HLA ligandome of tumor *versus* normal tissue.

Multiple HLA Ligands from One Source Protein—Table III lists mRNA and HLA presentation ratios of proteins that are highlighted in Fig. 4 and discussed below. Analysis of individual peptide pairs indicated tumor-associated changes in HLA presentation ratios (Table IV). For 20% of all proteins with several identified HLA ligands, HLA presentation ratios differed between the individual peptides more than 4-fold. For four peptides, N-terminally trimmed forms were identified (CCNI, HLA-B, RBBP4, and TMED10). The presentation ratios of these peptide variants changed up to 5-fold. This might indicate tumor-associated changes in antigen processing (34) and especially alterations in trimming by the ERAAP (9).

HLA Ligands Identified Only in One Tissue Specimen—Several HLA ligands were found to be presented exclusively on one tissue specimen (Table V), although mRNA ratios changed only marginally in most cases. Peptides derived from UDP-glucuronosyltransferase 1 family, polypeptide A6 (UGT1A6), uromodulin (UMOD), and the polymeric Ig receptor (PIGR) were presented uniquely on normal tissue (Fig. 4, *areas VII–IX*); peptides derived from annexin A4 (ANXA4), plexin B2

(PLXNB2), decycling heme oxygenase 1 (HMOX1), and adipophilin (ADFP) as well as from the small cell lung carcinoma cluster 4 antigen CD24 were presented solely on tumor tissue (Fig. 4, *areas II and III*). Peptides presented specifically on one tissue specimen might reflect both differences in antigen processing between one tumor/normal tissue pair and patient-specific variations: identical peptides from ANXA4 and ADFP were identified in different tumors but without being presented uniquely. For 60% of all source proteins in the group of the top 5% overexpressed peptides (Fig. 4, *areas I–III*), tumor association has been reported, and this number actually increases to nearly 80% for peptides presented exclusively on tumor tissue (Supplemental Table 4). As far as tumor immunotherapy is concerned, these uniquely presented peptides are excellent targets, but they also underline the importance of patient-specific adaptations in such an approach (9).

HLA Ligands without Corresponding mRNA—The fact that there are differences between the transcriptome and HLA ligandome becomes even more obvious when one considers that several peptides could be identified for which no mRNA was detectable in the respective tissues (Table VI). In RCC100, for example, the mRNA for the EH-domain-containing protein 2 (EHD2) was detectable neither in tumor nor in normal tissue. Nevertheless the EHD2-derived peptide ALASHLIEA was identified on tumor as well as on normal tissue (Fig. 2, *B–D*). These HLA ligands are presumably derived from long lived proteins from which the mRNA has already been degraded (36) or represent mutated peptides for which the correct allocation to the correct mRNA was not possible any more.

TABLE II
Gene chip analysis of gene transcripts involved in antigen processing

Analysis comprised constitutive proteasomal subunits (PSMB1, -2 and -5), immunoproteasomal subunits (LMP7, -2, and MECL1), subunits of the immunoproteasomal regulator PA28 (PSME1–3), proteins of the HLA peptide-loading complex (TAP1 and -2, tapasin, calreticulin, calnexin, and PDIA3), HLA classes I and II (HLA-A, -B, -C, -DR, -DP, and -DQ), the ERAAP, and proteins of the SEC61 translocon that can be involved in peptide export from the ER. Proteins inducible by interferon γ are highlighted in bold. histocomp., histocompatibility; cass., cassette; aminopep. assoc. w. antigen process., aminopeptidase associated with antigen processing.

Gene symbol	Gene title	log₂ mRNA ratio		
		RCC099	RCC100	RCC110
PSMB1	Proteasome subunit β1	0.4	0.4	0.6
PSMB2	Proteasome subunit β2	0.3	0.1	0.5
PSMB5	Proteasome subunit β3	0.0	−0.2	0.2
LMP7	**Proteasome subunit β8**	**2.5**	**2.1**	**2.5**
LMP2	**Proteasome subunit β9**	**1.8**	**1.7**	**3.5**
MECL1	**Proteasome subunit β10**	**1.3**	**0.8**	**2.4**
PSME1	**Proteasome activator subunit 1**	**0.2**	**0.2**	**0.7**
PSME2	**Proteasome activator subunit 2**	**0.1**	**−0.3**	**1.4**
PSME3	**Proteasome activator subunit 3**	**−0.1**	**−0.9**	**−0.6**
CALR	Calreticulin	0.0	0.0	0.1
CANX	Calnexin	1.5	0.8	2.0
TAP1	**Transporter 1, ATP-binding cass.**	**1.5**	**1.8**	**2.6**
TAP2	**Transporter 2, ATP-binding cass.**	**0.3**	**1.1**	**2.6**
TAPBP	**Tapasin**	**1.4**	**1.1**	**1.6**
HLA-A	**Major histocomp. complex I A**	**0.8**	**0.3**	**1.1**
HLA-B	**Major histocomp. complex I B**	**1.3**	**0.8**	**2.1**
HLA-C	**Major histocomp. complex I C**	**0.9**	**0.5**	**1.6**
HLA-DP	**Major histocomp. complex II DP**	**1.4**	**0.6**	**2.5**
HLA-DQ	**Major histocomp. complex II DQ**	**2.0**	**1.3**	**3.5**
HLA-DR	**Major histocomp. complex II DR**	**1.1**	**0.6**	**2.4**
PDIA3	Protein-disulfide isomerase A3	0.2	0.1	0.7
SEC61A1	Sec61 α1 subunit	0.6	−0.5	0.5
SEC61A2	Sec61 α1 subunit	0.0	−0.9	−1.2
SEC61B	Sec61 α1 subunit	−0.1	−0.2	0.6
SEC61G	Sec61 α1 subunit	1.9	0.9	1.2
ERAP1	**ER aminopep. assoc. w. antigen process.**	**0.7**	**0.7**	**0.8**

TABLE III
Diversity of peptide and RNA ratios highlighted by 11 examples

Genes were sorted according to the area classification introduced in Fig. 4. HLA ligand ratios and mRNA ratios were calculated between tumor and autologous normal tissue. Gene symbol and title can be found at www.ncbi.nlm.nih.gov/entrez/query.fcgi?db=gene.

Area	Gene symbol	Gene title	Sequence	log₂ HLA ligand ratio	log₂ mRNA ratio	Source
II	PLXNB2	Plexin B2	TYTDRVFFL	9.58	−0.50	RCC110
II	ADFP	Adipose differentiation-related protein	VRLGSLSTK	4.22	−0.08	RCC099
II	CD24	CD24 antigen	RAMVARLGL	5.32	0.5	RCC100
III	ANXA4	Annexin A4	DEVKFLTV	3.52	1.41	RCC100
III	ADFP	Adipose differentiation-related protein	SLLTSSKGQLQK	2.32	1.71	RCC100
III	ANXA4	Annexin A4	DEVKFLTV	1.95	2.20	RCC110
III	HMOX1	Heme oxygenase (decycling) 1	KIAQKALDL	2.30	3.70	RCC110
VI	ADFP	Adipose differentiation-related protein	VRLGSLSTK	−0.81	3.60	RCC110
VII	UMOD	Uromodulin	RAFSSLGLLK	−5.49	−7.19	RCC100
VIII	UGT1A6	UDP-glucuronosyltransferase 1 A6	ALGKIPQTV	−4.55	1.12	RCC099
IX	PIGR	Polymeric immunoglobulin receptor	FSVVINQLR	−4.73	1.72	RCC099

HLA Ligands Identified in Several Patient Samples—Peptides identified in more than one patient allowed the evaluation of patient-specific variations in mRNA expression ratios and HLA presentation ratios (Supplemental Table 5). More than 12% of the HLA-presented peptides exhibited a variation in the presentation level in different patients that was greater than 4-fold and included many of the significantly over- or underpresented peptides. The peptide VRLGSLSTK derived

from the tumor-associated antigen ADFP (37) was underpresented on RCC110, but mRNA levels were clearly up-regulated in the tumor tissue (Fig. 4, *area VI*). Yet the same peptide was presented exclusively on RCC099, although the mRNA levels of ADFP remained unchanged between tumor and normal tissue (Fig. 4, *area II*). Another different ADFP-derived peptide (SLLTSSKGQLQK) was presented on RCC100 by HLA-A*03 with an mRNA ratio that matched its HLA presen-

TABLE IV
Multiple peptides from one source protein identified in one tumor and normal tissue pair

HLA presentation ratios were calculated between a corresponding tumor and normal tissue pair. Peptides that were identified also in N-terminally trimmed forms are marked in bold. Gene symbol and title can be found at www.ncbi.nlm.nih.gov/entrez/query.fcgi?db=gene. elongat., elongation; histocomp., histocompatibility; Heterogen., heterogeneous; ribonucleoprot., ribonucleoprotein; bind. prot., binding protein; activ., activator.

Gene symbol	Gene title	Sequence	log₂ HLA ligand ratio	log₂ mRNA ratio	HLA restriction	Source
ALDOA	Aldolase A	ALSDHHIYL	3.38	2.72	A02	RCC099
ALDOA	Aldolase A	RTVPPAVTGITF	2.63	2.72	B57	RCC099
CCNI	Cyclin I	**LLDRFLATV**	-0.93	-0.18	A02	RCC099
CCNI	Cyclin I	**SLLDRFLATV**	0.01	-0.18	A02	RCC099
EEF2	Eukaryotic translation elongat. factor 2	ILTDITKGV	-0.91	0.42	A02	RCC099
EEF2	Eukaryotic translation elongat. factor 2	RRWLPAGDAL	0.37	0.42	B27	RCC099
FLNA	Filamin A	GTHKVTVLF	0.06	1.02	B57	RCC099
FLNA	Filamin A	GTHTVSVKY	1.01	1.02	B57	RCC099
FLNA	Filamin A	GVHTVHVTF	-0.24	1.02	B57	RCC099
GNB2L1	Guanine nucleotide-bind. prot. b2-like 1	KTIKLWNTL	1.06	1.02	A02	RCC099
GNB2L1	Guanine nucleotide-bind. prot. b2-like 1	YTDNLVRVW	0.24	1.02	B57	RCC099
HLA-A or -G	Major histocomp. complex I A or G	VMAPRTLLL	-0.23	1.60	A02	RCC110
HLA-A	Major histocomp. complex I A	VMAPRTLVL	0.40	1.60	A02	RCC110
HLA-B	Major histocomp. complex I B	**AAQITQRKW**	1.84	1.29	B57	RCC099
HLA-B	Major histocomp. complex I B	**TAAQITQRKW**	1.61	1.29	B57	RCC099
HNRPM	Heterogen. nuclear ribonucleoprot. M	KSRGIGTVTF	-0.74	0.47	B57	RCC099
HNRPM	Heterogen. nuclear ribonucleoprot. M	LLFDRPMHV	0.43	0.47	A02	RCC099
LMNA	Lamin A/C	KAGQVVTIW	0.29	0.07	B57	RCC099
LMNA	Lamin A/C	MRARMQQQL	-0.60	0.07	B27	RCC099
PPP1CA or -B or -C	Protein phosphatase 1α or b or c	KYPENFFLL	6.20	0.35	C	RCC110
PPP1CA	Protein phosphatase 1α	SIIGRLLEV	0.47	0.35	A02	RCC110
RBBP4 or -7	Retinoblastoma-binding protein 4 or 7	HTAKISDFSW	-0.13	0.14	B57	RCC099
RBBP4 or -7	Retinoblastoma-binding protein 4 or 7	TAKISDFSW	0.43	0.14	B57	RCC099
RPS16	Ribosomal protein S16	ISKALVAYY	1.12	0.82	B57	RCC099
RPS16	Ribosomal protein S16	KLLEPVLLL	1.09	0.82	A02	RCC099
SCD	Stearoyl-CoA desaturase	ARLPLRLFL	3.96	1.52	B27	RCC099
SCD	Stearoyl-CoA desaturase	ITAGAHRLW	1.50	1.52	B57	RCC099
SSR1	Signal sequence receptor	VLFRGGPRGLLAVA	-2.00	0.70	A02	RCC099
SSR1	Signal sequence receptor	VLFRGGPRGSLAVA	-2.42	0.70	A02	RCC110
SSR1	Signal sequence receptor	VLFRGGPRGSLAVA	0.89	0.37	A02	RCC099
SSR1	Signal sequence receptor	VLFRGGPRGSLAVA	-1.35	0.37	A02	RCC099
STAT3	Signal transducer and activ. of transcript. 3	EERIVGLF	0.10	-0.80	B18	RCC099
STAT3	Signal transducer and activ. of transcript. 3	EELQGKVSY	0.38	-0.80	B18	RCC110
TMED10	Transmembrane trafficking protein 10	**FLLGPRLVLA**	-0.91	-0.08	A02	RCC099
TMED10	Transmembrane trafficking protein 10	**LLGPRLVLA**	1.49	-0.08	A02	RCC099
TMEM66	Transmembrane protein 66	KGWDGYDVQW	0.39	0.72	B57	RCC099
TMEM66	Transmembrane protein 66	RRLDPIPQL	-3.55	0.72	B27	RCC099
TNS1	Tensin 1	HAKVLEFGW	0.81	0.32	B57	RCC099
TNS1	Tensin 1	FLIETGPRGV	0.45	0.32	A02	RCC099
VIM	Vimentin	NLAEDIMRL	0.27	1.82	A02	RCC099
VIM	Vimentin	NYIDKVRFL	1.02	1.82	C	RCC099

tation ratio (Fig. 4, *area III*). HLA peptide ratios exhibited stronger patient individual changes than mRNA ratios might indicate. This is due to the fact that changes in the HLA ligandome reflect not only mRNA ratio alterations but also changes in the degradome, which to some extent is conserved in the HLA ligandome (38).

DISCUSSION

Stable Isotope Labeling of ex Vivo Isolated MHC Molecules— Stable isotope labeling is the method of choice for protein

quantification and is widely used in proteomics. For ex vivo prepared MHC peptide samples the standard isotope labeling methods are either not feasible or are not applicable to the majority of MHC-bound peptides due to their amino acid composition. To overcome these impediments we have established the dNIC strategy; to our knowledge this is the first study using an isotope-based quantitative MS method for a large scale *ex vivo* comparison of the HLA ligandome of two tissue specimens. Patient samples were chosen for analysis according to two criteria: categorization of the RCCs into the clear cell type by

TABLE V
HLA ligands exclusively identified in either tumor or normal tissue

Values were calculated against background and sorted according to their HLA presentation ratio between tumor and autologous normal tissue. Gene symbol and title can be found at www.ncbi.nlm.nih.gov/entrez/query.fcgi?db=gene. histocomp., histocompatibility; bind. prot., binding protein; N/A, not assigned.

Gene symbol	Gene title	Sequence	$\log_2$ HLA ligand ratio	$\log_2$ mRNA ratio	HLA restriction	Source
PLXNB2	Plexin B2	TYTDRVFFL	9.58	0.00	C	RCC110
PPP1CA or -B or -C	Protein phosphatase 1α or b or c	KYPENFFLL	6.20	0.35	C	RCC110
CD24	CD24 antigen	RAMVARLGL	5.32	0.71	N/A	RCC110
SLC17A3	Solute carrier family 17, member 3	ARYGIALVL	4.86	0.62	B27	RCC099
ADFP	Adipose differentiation-related protein	VRLGSLSTK	4.22	−0.08	B27	RCC099
MAT1A or -2A	Methionine adenosyltransferase Iα or IIa	RRVLVQVSY	4.08	0.50	B27	RCC110
SCD	Stearoyl-CoA desaturase	ARLPLRLFL	3.96	1.52	B27	RCC099
ANXA4	Annexin A4	DEVKFLTV	3.52	1.41	B18	RCC100
POLR2C	Polymerase II peptide C, 33kDa	KLSDLQTQL	3.52	0.10	A02	RCC110
HMOX1	Heme oxygenase 1	KIAQKALDL	2.30	3.70	A02	RCC110
CXCL14	Chemokine ligand 14	RLLAAALLL	2.09	0.47	A02	RCC099
OGG1	8-Oxoguanine DNA glycosylase	VLADQWWTL	−3.07	0.17	A02	RCC099
MYL6	Myosin light polypeptide 6	FVRHLSG	−3.45	0.12	N/A	RCC099
GNB5	Guanine nucleotide-bind. protein, b5	ILFGHENRV	−3.72	−0.78	A02	RCC099
HLA-B or -C	Major histocomp. complex I B or C	DTAAQITQR	−4.41	1.58	A68	RCC110
RPL15	Ribosomal protein L15	EVILDPFHK	−4.51	−0.75	A68	RCC110
UGT1A6	UDP-glucuronosyltransferase 1 A6	ALGKIPQTV	−4.55	1.12	A02	RCC110
PIGR	Polymeric immunoglobulin receptor	FSVVINQLR	−4.73	1.72	A03	RCC099
UMOD	Uromodulin	RAFSSLGLLK	−5.49	−7.19	A03	RCC100
MYO1C	Myosin IC	FLDHVRTSF	−5.69	0.36	A03	RCC100

TABLE VI
HLA ligands identified from RCC099, RCC100, and RCC110 with no detectable mRNA in tumor and/or normal tissue

Values were calculated against background; mRNA detection was categorized by GCOS software as present (P), marginally present (M), or absent (A). Gene symbol and title can be found at www.ncbi.nlm.nih.gov/entrez/query.fcgi?db=gene. N/A, not applicable.

Gene symbol	Gene title	Sequence	$\log_2$ HLA ligand ratio	$\log_2$ mRNA ratio	Detection of mRNA Tumor	Detection of mRNA Normal	Source
CLIC5	Chloride intracellular channel 5	NLLPKLHVV	3.00	−2.75	A	P	RCC099
ACVRL1	Activin A receptor type II-like 1	SPRKGLLML	−0.65	3.01	P	A	RCC100
EHD2	EH-domain-containing 2	ALASHLIEA	1.07	3.32	A	A	RCC100
EHD2	EH-domain-containing 2	ALASHLIEA	1.82	3.41	P	A	RCC099
LSP1	Lymphocyte-specific protein 1	KLIDRTESL	0.39	1.90	P	A	RCC110
PLVAP	Plasmalemma vesicle-associated protein	KVKTLEVEI	0.50	0.52	P	A	RCC099
SRXN1	Sulfiredoxin 1 homolog	TLSDLRVYL	0.43	0.32	P	M	RCC099
WDR78	WD repeat domain 78	TSVVYDVAW	0.32	0.52	P	A	RCC099
ATOX1	ATX1 antioxidant protein 1 homolog	RVLNKLGGVK	−1.01	N/A	A	A	RCC099
CCDC21	Coiled-coil domain-containing 21	RLQMEGMQL	−1.14	N/A	A	A	RCC100
CYHR1	Cysteine/histidine-rich 1	HLGPEGRSV	−1.21	N/A	M	A	RCC099
DHX38	DEAH box polypeptide 38	VLFGLLREV	0.81	N/A	A	A	RCC099
FLJ32206	Hypothetical protein FLJ32206	GSHFISHLS	−0.89	N/A	A	A	RCC099
GBP4	Guanylate-binding protein 4	KRLGTLVVTY	−0.60	N/A	A	A	RCC099
KIAA1305	KIAA1305	TLADIIARL	−0.10	N/A	A	A	RCC099
RASL11A	RAS-like, family 11, member A	YLLPKDIKL	−0.37	N/A	A	A	RCC099

histology and the broadest possible overlap of the MHC alleles between the different patients. Tumor samples were taken from its central area; control samples were from renal cortex assessed as "normal" and as distant as possible from the tumor.

Individual Variances in Antigen Processing—In the three RCC tissue pairs analyzed in this study, each sample displays to some extent individual features regarding antigen processing. Apart from HLA mismatches, the activity of enzymes involved in antigen processing also varied. We found, for

example, varying mRNA levels of immunoproteasome subunits in the different samples (Table II). All individual variances in antigen processing summarize at the level of the MHC ligandome. For example, we detected ADFP-derived peptides ranging in their presentation from exclusive presentation on tumor tissue to equal presentation on tumor and normal tissue. These individual variances in MHC:peptide levels are one of the reasons why for example tumor vaccination studies can vary extremely in their outcome.

Four Major Hypotheses—The HLA ligandome is more complex in its variations than mRNA, but it is of far greater immunological relevance; it reflects a particularly complex aspect of systems biology that is exemplified here by a naturally occurring change in tissue (tumor genesis). The long and complex path from mRNA transcription to HLA presentation is reflected in our observation of a generally weak mRNA-HLA-ligand correlation. Four hypotheses can thus be deduced from Fig. 4.

First, HLA ligand generation implies that one mRNA species is able to account for several different peptides that differ in their presentation ratios and that are potentially presented by different HLA allotypes (Table IV).

Second, for more than 75% of all identified HLA ligands, we could detect no major differences in the HLA peptide repertoire (39) (Fig. 4, *areas IV–VI*), although immunoproteasomes were up-regulated on a transcriptional level. Assuming transcription of immunoproteasomal mRNA and activity of the immunoproteasomal subunits, this would limit the implication of the proteasome composition on the HLA ligandome in our *ex vivo* setting (36).

Third, several HLA ligands could be identified although no corresponding mRNA was detectable. In these cases HLA ligands might be derived either from long lived proteins or from mutated proteins for which the correct peptide-mRNA allocation was not possible.

Fourth, differences in HLA presentation without mRNA changes (Fig. 4, *areas II* and *VIII*) are due to altered peptide generation that can be triggered by several scenarios (40). Higher translation efficiency leads to a larger number of DRiPs, which are known to be a major source for HLA ligands (41). The amount of DRiPs from certain source mRNAs might also be elevated due to mutations in some of the mRNAs, distorting transcription and thus increasing DRiP formation (17). On the other hand, enhanced protein turnover increases the total amount of substrates for proteases such as the proteasome. Moreover proteolytic activity in the cytosol or ER can vary for some peptides when tumor and normal tissue are compared.

Context and Limitations of the Chosen Experimental Setting—The exact molecular mechanism responsible for alterations in the level of our *ex vivo* isolated MHC-peptide complex levels could not be deduced. This is due to the fact that these alterations are most probably not caused by one single change in the peptide generation pathway or in the antigen-processing machinery but are rather complex, multifactorial changes established during tumor genesis. Defining molecular mechanisms in a complex interaction network such as the antigen-processing machinery is in many cases not possible. In a recent study by Milner et al. (38), the turnover kinetics of MHC peptides was determined in a cell culture setting. Not even in this plain setting could the "simple" discrimination between short lived proteins and DRiPs clearly be made. In these experiments the only strong indication for MHC-peptide complexes derived from DRiPs was a biphasic turnover kinet-

ics in pulse-chase experiments using incorporation of iso-tope-labeled amino acids.

In 1999 and 2003 the first quantitative experiments were carried out to compare the yeast transcriptome with its proteome (2, 4). Here the authors showed only a weak correlation between transcriptome and proteome ($r = 0.45$). In our study, the correlation between transcriptome and HLA ligandome was even weaker ($r = 0.32$), which might reflect that the generation of HLA ligands is a pathway that begins only after mRNA transcription. At the present time, large scale data regarding the extent of correlation between proteome and HLA ligandome are not available. Taking into consideration that a major portion of the HLA ligandome is supposed to be derived from the transient proteome, that short lived proteins and DRiPs, one could expect an even weaker correlation between the HLA ligandome and the well quantifiable permanent proteome.

Summary and Outlook—mRNA-based identification of tumor-associated antigens is well established and widely used. As we could show in this study that mRNA levels alone do not adequately reflect cellular reality at the HLA level, our results have a direct impact on T-cell-based immunotherapy. We conclude that for the rational selection of appropriate tumor-specific T-cell targets, quantitative HLA ligand analysis contributes greatly to the benefits of quantitative transcriptome analysis; a combination of both strategies enables the identification of new target candidates and helps to avoid false positive targets. In summary, comparing changes in the transcriptome to those in the HLA ligandome of renal tumor *versus* normal tissue without further reflection is like comparing apples to oranges. Conveying this finding to RNA-based vaccination, which was shown to be a potent vaccine also against cancer (42), one cannot take for granted that every mRNA leads to actual peptide presentation on HLA molecules. Thus for each mRNA that is designed for vaccination, intensive individual *in vitro* tests are advisable. Our findings provide insight into tumor-associated changes in translation efficiency and protein turnover and provide immunologically relevant tumor information to a depth that could not be achieved before with hitherto existing standard techniques.

REFERENCES

1. Admon, A., Barnea, E., and Ziv, T. (2003) Tumor antigens and proteomics from the point of view of the major histocompatibility complex peptides. *Mol. Cell. Proteomics* **2,** 388–398

2. Gygi, S. P., Rochon, Y., Franza, B. R., and Aebersold, R. (1999) Correlation between protein and mRNA abundance in yeast. *Mol. Cell. Biol.* **19,** 1720–1730

3. Princiotta, M. F., Finzi, D., Qian, S. B., Gibbs, J., Schuchmann, S., Buttgereit, F., Bennink, J. R., and Yewdell, J. W. (2003) Quantitating protein synthesis, degradation, and endogenous antigen processing. *Immunity* **18,** 343–354

4. Washburn, M. P., Koller, A., Oshiro, G., Ulaszek, R. R., Plouffe, D., Deciu, C., Winzeler, E., and Yates, J. R., III (2003) Protein pathway and complex clustering of correlated mRNA and protein expression analyses in Saccharomyces cerevisiae. *Proc. Natl. Acad. Sci. U. S. A.* **100,** 3107–3112

5. Falk, K., Rotzschke, O., Stevanovic, S., Jung, G., and Rammensee, H. G. (1991) Allele-specific motifs revealed by sequencing of self-peptides eluted from MHC molecules. *Nature* **351,** 290–296

6. Zinkernagel, R. M., and Doherty, P. C. (1974) Immunological surveillance against altered self components by sensitised T lymphocytes in lymphocytic choriomeningitis. *Nature* **251,** 547–548

7. Wolfel, T., Van Pel, A., Brichard, V., Schneider, J., Seliger, B., Meyer zum Buschenfelde, K. H., and Boon, T. (1994) Two tyrosinase nonapeptides recognized on HLA-A2 melanomas by autologous cytolytic T lymphocytes. *Eur. J. Immunol.* **24,** 759–764

8. Rammensee, H. G., Weinschenk, T., Gouttefangeas, C., and Stevanovic, S. (2002) Towards patient-specific tumor antigen selection for vaccination. *Immunol. Rev.* **188,** 164–176

9. Weinschenk, T., Gouttefangeas, C., Schirle, M., Obermayr, F., Walter, S., Schoor, O., Kurek, R., Loeser, W., Bichler, K. H., Wernet, D., Stevanovic, S., and Rammensee, H. G. (2002) Integrated functional genomics approach for the design of patient-individual antitumor vaccines. *Cancer Res.* **62,** 5818–5827

10. Yajima, N., Yamanaka, R., Mine, T., Tsuchiya, N., Homma, J., Sano, M., Kuramoto, T., Obata, Y., Komatsu, N., Arima, Y., Yamada, A., Shigemori, M., Itoh, K., and Tanaka, R. (2005) Immunologic evaluation of personalized peptide vaccination for patients with advanced malignant glioma. *Clin. Cancer Res.* **11,** 5900–5911

11. Hanash, S., Brichory, F., and Beer, D. (2001) A proteomic approach to the identification of lung cancer markers. *Dis. Markers* **17,** 295–300

12. van der Bruggen, P., Traversari, C., Chomez, P., Lurquin, C., De Plaen, E., Van den Eynde, B., Knuth, A., and Boon, T. (1991) A gene encoding an antigen recognized by cytolytic T lymphocytes on a human melanoma. *Science* **254,** 1643–1647

13. Takahashi, M., Rhodes, D. R., Furge, K. A., Kanayama, H., Kagawa, S., Haab, B. B., and Teh, B. T. (2001) Gene expression profiling of clear cell renal cell carcinoma: Gene identification and prognostic classification. *Proc. Natl. Acad. Sci. U. S. A.* **98,** 9754–9759

14. Mathiassen, S., Lauemoller, S. L., Ruhwald, M., Claesson, M. H., and Buus, S. (2001) Tumor-associated antigens identified by mRNA expression profiling induce protective anti-tumor immunity. *Eur. J. Immunol.* **31,** 1239–1246

15. Baumeister, W., Walz, J., Zuhl, F., and Seemuller, E. (1998) The proteasome: paradigm of a self-compartmentalizing protease. *Cell* **92,** 367–380

16. Yewdell, J. W., Anton, L. C., and Bennink, J. R. (1996) Defective ribosomal products (DRiPs): a major source of antigenic peptides for MHC class I molecules? *J. Immunol.* **157,** 1823–1826

17. Schubert, U., Anton, L. C., Gibbs, J., Norbury, C. C., Yewdell, J. W., and Bannink, J. R. (2000) Rapid degradation of a large fraction of newly synthesized proteins by proteasomes. *Nature* **404,** 770–774

18. Shepherd, J. C., Schumacher, T. N., Ashton-Rickardt, P. G., Imaeda, S., Ploegh, H. L., Janeway, C. A., Jr., and Tonegawa, S. (1993) TAP1-dependent peptide translocation in vitro is ATP dependent and peptide selective. *Cell* **74,** 577–584

19. Serwold, T., Gonzalez, F., Kim, J., Jacob, R., and Shastri, N. (2002) ERAAP customizes peptides for MHC class I molecules in the endoplasmic reticulum. *Nature* **419,** 480–483

20. Gaczynska, M., Rock, K. L., and Goldberg, A. L. (1993) γ-Interferon and expression of MHC genes regulate peptide hydrolysis by proteasomes. *Nature* **365,** 264–267

21. Hisamatsu, H., Shimbara, N., Saito, Y., Kristensen, P., Hendil, K. B., Fujiwara, T., Takahashi, E., Tanahashi, N., Tamura, T., Ichihara, A., and Tanaka, K. (1996) Newly identified pair of proteasomal subunits regulated reciprocally by interferon γ. *J. Exp. Med.* **183,** 1807–1816

22. Banchereau, J., Palucka, A. K., Dhodapkar, M., Burkeholder, S., Taquet, N., Rolland, A., Taquet, S., Coquery, S., Wittkowski, K. M., Bhardwaj, N., Pineiro, L., Steinman, R., and Fay, J. (2001) Immune and clinical responses in patients with metastatic melanoma vaccinated with CD34(+) progenitor-derived dendritic cell vaccine. *Cancer Res.* **61,** 6451–6458

23. Slingluff, C. L., Jr., Petroni, G. R., Yamshchikov, G. V., Hibbitts, S., Grosh, W. W., Chianese-Bullock, K. A., Bissonette, E. A., Barnd, D. L., Deacon, D. H., Patterson, J. W., Parekh, J., Neese, P. Y., Woodson, E. M., Wiernasz, C. J., and Merrill, P. (2004) Immunologic and clinical outcomes of vaccination with a multiepitope melanoma peptide vaccine plus low-dose interleukin-2 administered either concurrently or on a delayed schedule. *J. Clin. Oncol.* **22,** 4474–4485

24. Boer, J. M., Huber, W. K., Sultmann, H., Wilmer, F., von Heydebreck, A., Haas, S., Korn, B., Gunawan, B., Vente, A., Fuzesi, L., Vingron, M., and Poustka, A. (2001) Identification and classification of differentially expressed genes in renal cell carcinoma by expression profiling on a global human 31,500-element cDNA array. *Genome Res.* **11,** 1861–1870

25. Lovisolo, J. A., Casati, B., Clerici, L., Marafante, E., Bono, A. V., Celato, N., and Salvadore, M. (2006) Gene expression profiling of renal cell carcinoma: a DNA macroarray analysis. *BJU Int.* **98,** 205–216

26. Lemmel, C., Weik, S., Eberle, U., Dengjel, J., Kratt, T., Becker, H. D., Rammensee, H. G., and Stevanovic, S. (2004) Differential quantitative analysis of MHC ligands by mass spectrometry using stable isotope labeling. *Nat. Biotechnol.* **22,** 450–454

27. Schirle, M., Keilholz, W., Weber, B., Gouttefangeas, C., Dumrese, T., Becker, H. D., Stevanovic, S., and Rammensee, H. G. (2000) Identification of tumor-associated MHC class I ligands by a novel T cell-independent approach. *Eur. J. Immunol.* **30,** 2216–2225

28. Weinzierl, A. O., and Stevanovic, S. (2006) LC-MS-based protein and peptidequantification using stable isotope labels: from iCAT in general to differential N-terminal coding (dN2C) in particular, in *Biotechnology and Genetic Engineering Reviews* (Harding, S. E., ed) Vol. 23, pp 21–39, Lavoisier/Intercept, Cachan, France

29. Krüger, T., Schoor, O., Lemmel, C., Kraemer, B., Reichle, C., Dengjel, J., Weinschenk, T., Muller, M., Hennenlotter, J., Stenzl, A., Rammensee, H. G., and Stevanovic, S. (2005) Lessons to be learned from primary renal cell carcinoma: novel tumor antigens and HLA ligands for immunotherapy. *Cancer Immunol. Immunother.* **54,** 826–836

30. Gasti, G., Ebert, T., Finstad, C. L., Sheinfeld, J., Gomahr, A., Aulitzky, W., and Bander, N. H. (1996) Major histocompatibility complex class I and class II expression in renal cell carcinoma and modulation by interferon γ. *J. Urol.* **165,** 361–367

31. Toes, R. E., Nussbaum, A. K., Degermann, S., Schirle, M., Emmerich, N. P., Kraft, M., Laplace, C., Zwinderman, A., Dick, T. P., Muller, J., Schonfisch, B., Schmid, C., Fehling, H. J., Stevanovic, S., Rammensee, H. G., and Schild, H. (2001) Discrete cleavage motifs of constitutive and immunoproteasomes revealed by quantitative analysis of cleavage products. *J. Exp. Med.* **194,** 1–12

32. Basler, M., Youhnovski, N., Van Den Broek, M., Przybylski, M., and Groettrup, M. (2004) Immunoproteasomes down-regulate presentation of a subdominant T cell epitope from lymphocytic choriomeningitis virus. *J. Immunol.* **173,** 3925–3934

33. Chapiro, J., Claverol, S., Piette, F., Ma, W., Stroobant, V., Guillaume, B., Gairin, J. E., Morel, S., Burlet-Schiltz, O., Monsarrat, B., Boon, T., and Van den Eynde, B. J. (2006) Destructive cleavage of antigenic peptides either by the immunoproteasome or by the standard proteasome results in differential antigen presentation. *J. Immunol.* **176,** 1053–1061

34. Van der Bruggen, P., and Van den Eynde, B. J. (2006) Processing and presentation of tumor antigens and vaccination strategies. *Curr. Opin. Immunol.* **18,** 98–104

35. Hammer, G. E., Gonzalez, F., Champsaur, M., Cado, D., and Shastri, N. (2006) The aminopeptidase ERAAP shapes the peptide repertoire displayed by major histocompatibility complex class I molecules. *Nat. Immunol.* **7,** 103–112

36. Yewdell, J. W. (2005) The seven dirty little secrets of major histocompatibility complex class I antigen processing. *Immunol. Rev.* **207,** 8–18

37. Schmidt, S. M., Schag, K., Muller, M. R., Weinschenk, T., Appel, S., Schoor, O., Weck, M. M., Grunebach, F., Kanz, L., Stevanovic, S., Rammensee,

H. G., and Brossart, P. (2004) Induction of adipophilin-specific cytotoxic T lymphocytes using a novel HLA-A2-binding peptide that mediates tumor cell lysis. *Cancer Res.* **64**, 1164–1170

38. Milner, E., Barnea, E., Beer, I., and Admon, A. (2006) The turnover kinetics of major histocompatibility complex peptides of human cancer cells. *Mol. Cell. Proteomics* **5**, 357–365

39. van Hall, T., Sijts, A., Camps, M., Offringa, R., Melief, C., Kloetzel, P. M., and Ossendorp, F. (2000) Differential influence on cytotoxic T lymphocyte epitope presentation by controlled expression of either proteasome immunosubunits or PA28. *J. Exp. Med.* **192**, 483–494

40. Atkins, D., Ferrone, S., Schmahl, G. E., Storkel, S., and Seliger, B. (2004) Down-regulation of HLA class I antigen processing molecules: an immune escape mechanism of renal cell carcinoma? *J. Urol.* **171**, 885–889

41. Yewdell, J. W., Schubert, U., and Bennink, J. R. (2001) At the crossroads of cell biology and immunology: DRiPs and other sources of peptide ligands for MHC class I molecules. *J. Cell Sci.* **114**, 845–851

42. Scheel, B., Aulwurm, S., Probst, J., Stitz, L., Hoerr, I., Rammensee, H. G., Weller, M., and Pascolo, S. (2006) Therapeutic anti-tumor immunity triggered by injections of immunostimulating single-stranded RNA. *Eur. J. Immunol.* **36**, 2807–2816

Differential quantitative analysis of MHC ligands by mass spectrometry using stable isotope labeling

Claudia Lemmel[1], Steffen Weik[2], Ute Eberle[1], Jörn Dengjel[1], Thomas Kratt[3], Horst-Dieter Becker[3], Hans-Georg Rammensee[1] & Stefan Stevanović[1]

Currently, no method allows direct and quantitative comparison of MHC-presented peptides in pairs of samples, such as transfected and untransfected, tumorous and normal or infected and uninfected tissues or cell lines. Here we introduce two approaches that use isotopically labeled reagents to quantify by mass spectrometry the ratio of peptides from each source. The first method involves acetylation[1] and is both fast and simple. However, higher peptide recoveries and a finer sensitivity are achieved by the second method, which combines guanidination[2] and nicotinylation[3], because the charge state of peptides can be maintained. Using differential acetylation, we identified a beta catenin–derived peptide in solid colon carcinoma overpresented on human leucocyte antigen-A (HLA-A)*6801. Guanidination/nicotinylation was applied to keratin 18–transfected cells and resulted in the characterization of the peptide RLASYLDRV (HLA-A*0201), exclusively presented on the transfectant. Thus, we demonstrate methods that enable a pairwise quantitative comparison leading to the identification of overpresented MHC ligands.

The general strategy for differential MHC quantification is shown in Figure 1. Peptides from two different sources are derivatized either by an isotopically light reagent (hydrogen-containing) or an isotopically heavy reagent (deuterium-containing) to achieve different masses but the same physico-chemical behavior for the same peptide sequences. The two peptide derivatives are combined and separated by chromatography (either offline high performance liquid chromatography (HPLC) or online liquid chromatography mass spectrometry (LCMS)). Electrospray ionization mass spectrometry (ESI-MS) is used to achieve greater accuracy in differential ligand quantification. Sequence information is then determined by tandem mass spectrometry (MS/MS) and interpretation of fragment spectra using computer-assisted database searching tools.

First, we established an acetylation method using a synthetic peptide mixture of nonamers and decamers corresponding to normal MHC class I ligands. The modification procedure was optimized to obtain complete acetylation at the N terminus. Within 15 min, we obtained peptides fully acetylated at the N terminus, although partial
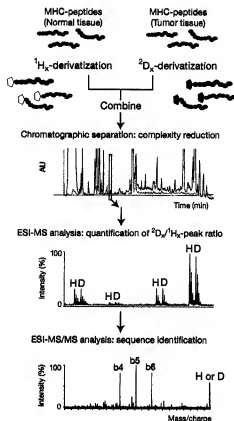
derivatization of the ε-amino group in lysine-containing peptides also occurred (data not shown).

We demonstrated the applicability of this method for differential acetylation of natural MHC class I ligands using an HPLC-fraction of HLA class I eluted peptides from MGAR cells. The peptide fraction was divided into two parts, one acetylated with $^1H_6$-acetic anhydride, the other with $^2D_6$-acetic anhydride, and after equimolar mixing the ratios of $^1H_3$-derivatized to $^2D_3$-derivatized peptides were determined. Figure 2 shows an example of the $^1H_3$-acetylated and $^2D_3$-acetylated variants of the peptide EVNGLISMY (MW 1040.5 Da) derived from the U5 small nuclear ribonucleoprotein–specific protein with a $^2D_3/^1H_3$ ratio of 1.0. For 15 additional peptides, detected as singly or doubly charged ions, the mean signal ratio was 1.01 and s.d. = 0.13 (see Supplementary Table 1 online). The acetylation procedure not only allows differential quantification of MHC ligands from two different sources but also greatly simplifies interpretation of MS/MS spectra of $^1H_3$-acetylated and $^2D_3$-acetylated peptide species. Owing to the 3-Da shift of the b-series ions, N- and C-terminal fragments can be easily distinguished when both species are present[4] (Fig. 2c). Unlike tryptic fragments labeled by isotope-coded affinity tag (ICAT), most MHC ligands do not carry a C-terminal lysine or arginine, and therefore the loss in sensitivity is quite severe for doubly charged ions because the acetyl group impedes the formation of a positively charged N terminus (signal displacement to singly charged ions occurs; data not shown). Usually, sequences occurring as singly charged ions yield signals of much lower intensity than those occurring as doubly charged ions (see Supplementary Table 1 online). Additionally, a signal distribution due to partial acetylation of the ε-amino group of lysines was observed in both $^1H_3$-acetylated and $^2D_3$-acetylated peptides, resulting in lower intensity of a given signal; however, this did not affect quantitative comparison because both species are affected to the same degree under stringently controlled experimental conditions. Nevertheless, this method is quick, easy to perform and reliable.

Using this differential acetylation approach, we modified peptide pools extracted from HLA class I molecules of solid colon carcinoma and regular colon tissue samples of comparable size by $^2D_3$-acetylation and $^1H_3$-acetylation of N termini, respectively, and then combined the samples. After peptide separation by microbore-HPLC, nineteen natural HLA ligands were identified by nanospray ESI-MS/MS analyses.

MHC-peptides (Normal tissue)   MHC-peptides (Tumor tissue)

^{1}H$_x$-derivatization ^{2}D$_x$-derivatization

Combine

Chromatographic separation: complexity reduction

ESI-MS analysis: quantification of ^{2}D$_x$/^{1}H$_x$-peak ratio
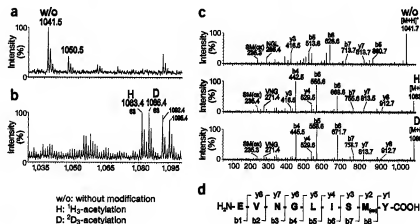
ESI-MS/MS analysis: sequence identification

Figure 1 Strategy for differential quantification of MHC-eluted peptides. MHC ligands derived from two different sources (e.g., tumor and normal tissue) are N-terminally derivatized either by a ^{1}H$_x$- or ^{2}D$_x$-reagent (reagents: acetic anhydride; Nic-NHS ester) and combined. After reduction of the peptide complexity by HPLC, peptides are quantified by ESI-MS analysis according to their peak areas. A pair of derivatized peptides (H, ^{1}H$_x$-derivatization; D, ^{2}D$_x$-derivatization) is physico-chemically identical and easily detectable because it essentially coelutes in chromatographic systems. Furthermore, there is a constant mass difference measured in the mass spectrometric scans. The difference depends on the number of stable isotopes in the derivative ([M+H]$^+$: acetylation: 3 Da; nicotinylation: 4 Da; [M+2H]$^{2+}$: acetylation: 1.5 Da; nicotinylation: 2 Da). Sequence identification of a ligand is revealed by ESI-MS/MS analysis and computer-assisted database search of the spectrum recorded.

interval of 0.87 to 2.56. The two overpresented HLA ligands are derived from ribosomal protein L24 and beta-catenin. Although little data exist on the potential tumor association of ribosomal protein L24, it has been reported that ribosomal proteins might play a role in carcinogenesis, for example L15 in esophageal carcinoma[5]. Beta-catenin functions as an oncogene by transactivating other oncogenes, including MMP-7, a metalloproteinase involved in metastasis development[6]. It also acts as a transcriptional coactivator in Wnt signaling, and its nuclear accumulation is critical for activation of the Wnt transcriptional response[7–9]. Genetic manipulations that perturb nuclear localization of beta-catenin lead to a loss of proliferative capacity in colon cancer cells[10]. A number of natural HLA ligands from beta-catenin are listed in the SYFPEITHI database[11] (http://www.syfpeithi.de/). A mutated beta-catenin peptide has been defined to function as a target of HLA-A*24-restricted, melanoma-specific, tumor-infiltrating lymphocytes[12].
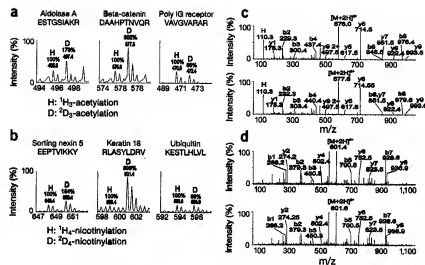
Because the acetylation method results in a substantial loss of sensitivity in peptides without C-terminal charge, we used a combination of two derivatization methods. For the first step, lysine side chains were completely guanidinated by O-methyl isourea hemisulfate[2] for a uniform derivatization of all ε-amino groups without modification of the N termini (data not shown)[13]. In a second modification step, all N termini were nicotinylated with nicotinoyloxy succinimide (Nic-NHS) reagent to maintain the charge state of the peptides[3]. This reaction was done on a C$_{18}$ microcolumn, which also allowed quick desalting before mass spectrometric analysis. Four synthetic peptides were used to optimize the combination of the derivatization methods on MHC-presented peptides. Nicotinylation of tyrosines was the only side reaction observed but was reversed immediately by hydroxy-

Seventeen peptides could be differentially quantified (see Supplementary Table 2 online). Most of these peptides were present in comparable amounts in both tissues, yielding ratios from 1.07 to 2.42. The overall peptide presentation in tumor tissue was 1.7-fold higher than in normal tissue (mean value 1.71, Fig. 3a (left panel)). Two peptides showed overpresentation in tumor tissue (one example shown in Fig. 3a (central panel)) and one peptide was underpresented (Fig. 3a (right panel)). MS/MS spectra of both ^{1}H$_3$-acetylated and ^{2}D$_3$-acetylated DAAHPTNVQR are shown in Figure 3c. Applying the student t-test to the quantified ligands, only the three over- or underpresented ligands are not contained within a 99.99% confidence

a w/o
1041.5
1050.5

b
H   H   1083.4 1084.4
D   D
1085.1
1086.1

1,035   1,050   1,065   1,080   1,095

w/o: without modification
H: ^{1}H$_3$-acetylation
D: ^{2}D$_3$-acetylation

c w/o
1041.7

H [M+H]$^+$
1044.7

D [M+H]$^+$
1088.6

100 200 300 400 500 600 700 800 900 1,000

d
$$H_2N-E-V-N-G-L-I-S-M_{ox}-Y-COOH$$

Figure 2 MS spectra before and after acetylation. (a,b) Mass spectra of nonmodified (a) and ^{1}H$_3$-/^{2}D$_3$-acetylated (b) HLA peptides eluted from MGAR cells. A peptide fraction was divided into two equal parts before differential acetylation and afterwards combined for nanospray ESI-MS analysis. (c) Fragment spectra of [M+H]$^+$ of three species of the peptide EVNGLISMY: nonmodified, ^{1}H$_3$-acetylated and ^{2}D$_3$-acetylated. (d) Nomenclature of fragment ions.

Figure 3 Differential quantification of HLA ligands derived from two different sources. (a) Mass spectra of $^2D_3$-acetylated HLA peptides from colon carcinoma compared to $^1H_3$-acetylated HLA peptides from regular colon tissue. Example of a peptide with average $^2D_3/^1H_3$ ratio (left); peptide overpresented in colon carcinoma (middle); peptide underpresented in colon carcinoma (right). (b) Mass spectra of guanidinated $^1H_3$-nicotinylated HLA peptides from Awells cells compared to guanidinated $^2D_4$-nicotinylated HLA peptides from keratin 18–transfected Awells cells. Peptide equally presented in both cell types (left); peptide overpresented in keratin 18 transfectant (middle); peptide with the lowest $^2D_4/^1H_4$ ratio determined in this experiment (right). (c) MS/MS spectra of $^1H_3$-acetylated (upper) and $^2D_3$-acetylated (lower) DAAHPTNVQR. (d) MS/MS spectra of $^2D_4$-nicotinylated synthetic RLASYLDRV (upper) in comparison to the $^2D_4$-nicotinylated natural sequence (lower).
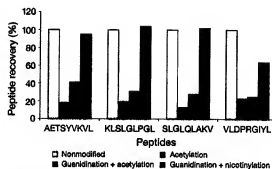
lamine treatment (data not shown). The strong impact of acetylation or guanidination/nicotinylation on peptide ionization can be partially compensated for by guanidination in lysine-containing peptides. The largest effect on ionization is caused by N-terminal nicotinylation, which leads to peptide recoveries similar to those of nonmodified peptides (**Fig. 4**). To determine whether guanidination/nicotinylation is generally applicable to quantification of HLA-presented peptides, we used a peptide pool obtained after immunoprecipitation of HLA-A*0201 molecules of C1R-A2 cells. After guanidination of ε-amines of lysine residues, this peptide pool was divided into two parts, modified separately by $^2D_4$- or $^1H_4$-nicotinylation, respectively, and combined again. After peptide separation by microbore HPLC, 19 natural ligands were identified in the HPLC fractions by nanospray ESI-MS/MS. The mean value of peptide ratio for $^2D_4$ Nic-/$^1H_4$ Nic-peptide was 1.00, s.d. = 0.12, a value slightly better than that achieved with acetylation (data not shown).

To identify ligands presented exclusively by certain cells, we used guanidination and $^2D_4$-/$^1H_4$-nicotinylation for the identification and quantification of HLA-ligand pools from the cell line Awells and its keratin 18 transfectant. Keratins have been suggested as markers that distinguish normal and tumor-derived cells[14]. More specifically, keratin 18 can be tumor-associated and overexpressed in carcinomas[15,16]. Therefore, our interest has been directed towards this protein[17], and transfectants were used to identify new HLA ligands of this protein. Two peptide pools extracted from HLA class I molecules of Awells–keratin 18 and Awells were derivatized by guanidination and by N-terminal $^2D_4$-nicotinylation and $^1H_4$-nicotinylation, respectively. The labeled peptide pools were combined and quantified in a

first experiment by online-microcapillary LCMS. In a second MS/MS experiment, 27 peptide sequences were identified (see Supplementary Table 3 online). All peptides were presented within the confidence interval on both nontransfected and transfected cells (**Fig. 3b** (left panel)), with the exception of one peptide with a MW of 1091.6 Da (**Fig. 3b** (central panel)). The sequence was identified as RLASYLDRV, which is a peptide derived from keratin 18. MS/MS spectra of RLASYL-DRV and its synthetic counterpart are shown in **Figure 3d**. There was no $^1H_4$ signal detectable in the background, indicating exclusive presentation of the keratin 18–derived ligand in the keratin-transfected cells. For this reason an exact ratio could not be determined; however, the signal of the deuterated peptide was at least six times greater than the background value. The peptide with the lowest ratio is shown in **Figure 3b** (right panel); however it is not significantly underpresented on the transfected Awells cells. It is contained within the confidence interval 0.64 to 2.28 obtained using the student t-test.

Both the acetylation and guanidination/ nicotinylation methods described above are aimed at quantitative investigation of MHC ligand presentation. Since early, pioneering work[18], there have been many attempts to detect and quantify differences in MHC-presented peptides of sample pairs by various mass spectrometric methods. For example, after using proteasome inhibitors, the pattern of HLA ligands has been compared to native cells[19], and upregulation of abundant self-peptides after viral infection has been investigated by HPLC-MS[20]. Matrix-assisted laser desorption ionization/time-of-flight technology has been used to analyze quantitative differences between peptide pools presented by closely related HLA allelic products[21]. None of the reported strategies, however, enables the fast detection of exact quantitative differences of larger numbers of sequences that were previously unknown. We propose isotope labeling as the method of choice for such investigations. The acetylation procedure is simple and quick compared with derivatization by guanidination/nicotinylation. However, successful application of N-terminal acetylation is restricted to MHC-eluted peptides containing basic amino acids at the C-terminal anchor to maintain analytical sensitivity during MS analysis. The analysis of guanidinated and nicotinylated peptides is as sensitive as the analysis of nonderivatized peptides. Thus, the two methods can be used alternatively according to the sample characteristics for relative quantification of MHC ligands from two different sources.

There is a chromatographic isotope effect when using deuterium for stable isotope labeling: early in the elution of a peak, the deuterated species is enriched, whereas at the tailing edge of a peak the protonated peptide variant prevails. This effect increases with the number of deuterium atoms contained in the reagent[22]. Thus, acetylated (D_3) or nicotinylated (D_4) peptides exhibit a higher degree of coelution than peptides containing the classical ICAT reagent with eight deuterium atoms. A second generation of ^{13}C ICAT reagent has been developed to optimize the coelution[23]. Unfortunately, reagents for the synthesis of a ^{13}C-containing Nic-NHS reagent, which would likewise not

Figure 4 Recoveries of different peptide derivatives. The four synthetic peptides (AETSYVKVL, KLSLGLPGL, SLGLQLAKV and VLDPRGIYL) present in equimolar concentrations were either acetylated, acetylated/guanidinated or guanidinated/nicotinylated. After complete derivatization, each peptide mixture was combined with the initial nonmodified peptide mixture (thus expecting equimolar yields of both species) and quantified by nanospray-ESI MS analysis.

exhibit a chromatographic isotope effect, are not yet commercially available.

Our results show that by pairwise quantitative analysis of MHC ligands, we can detect potential tumor-associated (that is, overexpressed) antigens by the greater abundance of their HLA ligands and potential tumor-specific (that is, exclusively expressed) antigens by the existence of single peptide species. The identification of new tumor-associated antigens is usually done with quantitative screening methods such as gene expression analysis or proteome analysis. It is a long way, however, from mRNA or protein expression levels to MHC ligands, involving the specificity steps of proteasomal processing, transporter-associated-with-antigen-processing (TAP) transport and MHC binding. Future studies of the correlation between differential quantification of MHC ligands using our approach and gene expression profiling or other methods would be of interest.

METHODS

Materials. Reagents for synthesis and derivatization, such as acetic-^{1}H$_6$-anhydride, O-methyl isourea hemisulfate, nicotinic acid ethyl ester, N-hydroxy succinimide, EDC N-(3-dimethylaminopropyl)-N'-ethyl-carbodiimide hydrochloride and hydroxyl amine, were purchased from Fluka. Acetic-^{2}D$_6$-anhydride was purchased from Sigma-Aldrich, ^{2}D$_4$-nicotinic acid ethyl ester was purchased from LGC Promochem. The HPLC reagents, trifluoroacetic acid, acetonitrile, formic acid and HPLC water, were purchased from Merck.

Synthesis of the 1-([^{1}H$_4$/^{2}D$_4$] nicotinyloxy)succinimide (^{1}H$_4$/^{2}D$_4$-Nic-NHS) esters. ^{1}D$_4$-nicotinic acid ethyl ester (5 g, 32.2 mmol) was dissolved in ethanol/water (1:1, 32 ml). Sodium hydroxide (1.53 g, 38.1 mmol) was added and the solution refluxed over night. After removal of ethanol by evaporation the solution was diluted with water (40 ml) and extracted with diethylether (32 ml). The aqueous phase was neutralized with concentrated HCl and pH was adjusted to 4–4.5. The resulting precipitate was filtered and washed with cold water and ether. Aqueous washings and mother lye were combined, adjusted to pH 2.8 and evaporated to dryness. The residue was redissolved in 1 N HCl (as little as possible) and adjusted to pH 3.5 with saturated NaOH. The resulting precipitate was filtered and washed with cold water and ether. Combination of the precipitates yielded ^{1}D$_4$-nicotinic acid as a white powder (3.11 g, 76%). Thus obtained, ^{1}D$_4$-nicotinic acid (3.11 g, 24.5 mmol) was suspended in dry CH$_2$Cl$_2$ (150 ml). N-(3-dimethylaminopropyl)-N'-ethyl-carbodiimid hydrochloride (EDC) (5.18 g, 27 mmol) and N-hydroxy succinimide (3.53 g, 30.63 mmol) were added and the resulting solution stirred overnight at 22 C. The reaction mixture was extracted with saturated sodium bicarbonate

solution (75 ml) and water (75 ml) and the organic phase was dried (NaSO$_4$). Evaporation of the solvent in vacuo yielded the ^{1}H$_4$/^{2}D$_4$-Nic-NHS ester (5.06 g, 92%). Purity and structure were confirmed by ^{1}H- and ^{13}C-NMR.

Peptides. Synthetic peptides were synthesized in an automated peptide synthesizer 432A (Applied Biosystems) following the 9-fluorenylmethyl-oxocarbony/tert-butyl (Fmoc/tBu) strategy as described[24].

Elution of HLA-presented peptides. HLA peptides were obtained by immune precipitation of HLA molecules from cell lines (HLA-defined human B-lymphoblastoid lines CIR-A2, International Histocompatibility Workshop (IHW) No. 9208; MGAR, IHW No. 9014; Awells, IHW No. 9090) or solid tissues according to a slightly modified protocol[25,26] using the pan-HLA-A,-B,-C-specific antibody W6/32, protein A-sepharose, acid treatment and ultrafiltration.

Transfection. The cDNA of keratin 18 was subcloned using TOPO TA cloning (Invitrogen) and inserted into the EcoRI and NotI sites of pcDNA3-Ii, in frame with the Ii sequence. Stable transfectants were generated by electroporation of Awells cells, followed by cloning using the limiting dilution method.

Acetylation of peptides. We added 10 µl ^{1}H$_6$-acetic anhydride or ^{2}D$_6$-acetic anhydride (50% (vol/vol) in methanol) to 100 µl peptide mixture (200 pmol to 2 nmol) in 50% methanol/water (vol/vol). The mixture was allowed to react at 22 C for 15 min. The reaction was stopped by addition of 1.1 µl of formic acid and equal aliquots of both samples were mixed.

Guanidination of peptides. Peptide mixtures (200 pmol to 2 nmol) in citrate buffer (50 mM; pH 3) containing 0.25% trifluoroacetic acid (TFA) (vol/vol) were adjusted to a pH of 10.5 with 200 µl sodium hydroxide (10 M). After addition of 1 ml freshly prepared O-methyl isourea hemisulfate solution (2.5 M in water) the mixture was incubated for 10 min at 65 C in a water bath. The reaction was stopped by adding 200 µl formic acid.

Nicotinylation of guanidinated peptides. Guanidinated peptides were loaded on a reversed phase C-18 microcolumn (Agilent Technologies hydrophobic 202-XGSXB) and washed with 0.5 ml water. The bound peptides were then modified by slowly passing 1 ml of freshly prepared ^{1}H$_4$- or ^{2}D$_4$-Nic-NHS ester (sodium phosphate buffer 50 mM; pH 8.5) through the column. The procedure was done twice before 1 ml of hydroxylamine was run through the column to remove tyrosine modifications. Finally, after washing with water, the modified peptides were eluted using 100 µl of 50% acetonitrile/water (vol/vol).

Offline HPLC separation. Modified peptide pools were mixed in equimolar amounts and the volume reduced to approximately 100 µl by vacuum centrifugation. The mixture was diluted with 400 µl water containing 0.08% TFA (vol/vol) before injecting the sample into a reversed phase SMART-HPLC system (Amersham). Labeled peptide mixtures were separated by gradient elution from a reversed-phase column (µRP SC C2/C18-column, 100   2.1 mm, Pharmacia). The samples were run through a binary gradient of 10–60% B within 100 min, applying a flow rate of 150 µl/min. Solvent A was 0.1% TFA/water (vol/vol). Solvent B contained 0.08% TFA in 80% acetonitrile/water (vol/vol). The peptides were fractionated in 150 µl aliquots. Before MS analysis each fraction was dried completely and resuspended in 50% methanol/0.1% formic acid.

Microcapillary LCMS. Synthetic and natural peptide mixtures were analyzed by a reversed phase Ultimate HPLC system (Dionex), coupled to a hybrid quadrupole orthogonal acceleration time-of-flight MS/MS (Q-TOF, Micromass)[27] equipped with a micro-ESI source. Samples were loaded onto a C$_{18}$ precolumn for concentration and desalting. After loading, the precolumn was placed in line for separation by a fused-silica microcapillary column (75 µm internal diameter   250 mm) packed with 5 µm C$_{18}$ reversed-phase material (Dionex). Solvent A was 4 mM ammonium acetate/water. Solvent B was 2 mM ammonium acetate in 80% acetonitrile/water. Both solvents were adjusted to pH 3 with formic acid. Samples were run through a binary gradient of 15–60% B within 120 min, applying a flow rate of 200 µl/min reduced to ~300 nl/min by the Ultimate split-system. A gold-coated glass capillary (PicoTip, New Objective) was used for introduction into the micro-ESI source.

The integration time for the TOF analyzer was 1 s with an interscan delay of 0.1 s. The ratios of deuterated and nondeuterated peptide species were calculated from the relative peak height.

For online microcapillary HPLC MS/MS experiments, the integration time for the TOF analyzer was 4 s with an interscan delay of 0.1 s. Fragmentation of parent ions $[M+H]^+$ or $[M+H]^{2+}$ was achieved by automatic switching between MS and MS/MS. Fragment spectra were analyzed manually and database searches (National Center for Biotechnology Information, Expressed Sequence Tag) were carried out using Multiple Alignment System for Protein Sequences Based on Three-way Dynamic Programming (MASCOT).

Nanoflow ESI-MS analysis and quantification. For sample introduction metal-coated glass capillaries (Proxeon) were used, working at flow rates of about 20 to 50 nl/min. The ratios of deuterated and nondeuterated peptide species were calculated from the relative peak heights as well as from peak area. For Nanoflow ESI MS/MS experiments, peptide ions were selected and fragmentation of $[M+H]^+$ and $[M+2H]^{2+}$ was carried out using collision energies of 30–60 eV and 20–30 eV, respectively. The integration time for the TOF analyzer was 1 s with an interscan delay of 0.1 s.

Note: Supplementary information is available on the Nature Biotechnology website.

1. Riordan, J.F. Acetylation. *Methods Enzymol.* **11**, 565–570 (1967).
2. Beardsley, R.L. & Reilly, J.P. Optimization of guanidination procedures for MALDI mass mapping. *Anal. Chem.* **74**, 1884–1890 (2002).
3. Munchbach, M., Quadroni, M., Miotto, G. & James, P. Quantitation and facilitated *de novo* sequencing of proteins by isotopic N-terminal labeling of peptides with a fragmentation-directing moiety. *Anal. Chem.* **72**, 4047–4057 (2000).
4. Ji, J. *et al.* Strategy for qualitative and quantitative analysis in proteomics based on signature peptides. *J. Chromatogr. B Biomed. Sci. Appl.* **745**, 197–210 (2000).
5. Wang, Q. *et al.* Cloning and characterization of full-length human ribosomal protein L15 cDNA which was overexpressed in esophageal cancer. *Gene* **263**, 205–209 (2001).
6. Ougolkov, A.V., Yamashita, K., Mai, M. & Minamoto, T. Oncogenic beta-catenin and MMP-7 (matrilysin) cosegregate in late-stage clinical colon cancer. *Gastroenterology* **122**, 60–71 (2002).
7. Bienz, M. & Clevers, H. Linking colorectal cancer to Wnt signaling. *Cell* **103**, 311–320 (2000).
8. Bienz, M. & Clevers, H. Armadillo/beta-catenin signals in the nucleus—proof beyond a reasonable doubt? *Nat. Cell Biol.* **5**, 179–182 (2003).
9. Zechner, D. *et al.* Beta-catenin signals regulate cell growth and the balance between progenitor cell expansion and differentiation in the nervous system. *Dev. Biol.* **258**, 406–418 (2003).
10. Shih, I.M., Yu, J., He, T.C., Vogelstein, B. & Kinzler, K.W. The beta-catenin binding domain of adenomatous polyposis coli is sufficient for tumor suppression. *Cancer Res.* **60**, 1671–1676 (2000).
11. Rammensee, H., Bachmann, J., Emmerich, N.P., Bachor, O.A. & Stevanovic, S. SYFPEITHI: database for MHC ligands and peptide motifs. *Immunogenetics* **50**, 213–219 (1999).
12. Robbins, P.F. *et al.* A mutated beta-catenin gene encodes a melanoma-specific antigen recognized by tumor infiltrating lymphocytes. *J. Exp. Med.* **183**, 1185–1192 (1996).
13. Kimmel, J.R. Analysis of homoarginine. *Methods Enzymol.* **11**, 584–589 (1967).
14. Trask, D.K. *et al.* Keratins as markers that distinguish normal and tumor-derived mammary epithelial cells. *Proc. Natl. Acad. Sci. USA* **87**, 2319–2323 (1990).
15. Fossar, N., Chaouche, M., Prochasson, P., Rousset, M. & Brison, O. Deregulated expression of the keratin 18 gene in human colon carcinoma cells. *Somat. Cell Mol. Genet.* **25**, 223–235 (1999).
16. Chu, Y.W., Seftor, E.A., Romer, L.H. & Hendrix, M.J. Experimental coexpression of vimentin and keratin intermediate filaments in human melanoma cells augments motility. *Am. J. Pathol.* **148**, 63–69 (1996).
17. Weinscheck, T. *et al.* Integrated functional genomics approach for the design of patient-individual antitumor vaccines. *Cancer Res.* **62**, 5818–5827 (2002).
18. Hunt, D.F. *et al.* Characterization of peptides bound to the class I MHC molecule HLA-A2.1 by mass spectrometry. *Science* **255**, 1261–1263 (1992).
19. Luckey, C.J. *et al.* Proteasomes in the expression of human class I MHC alleles and their associated peptides in the presence of proteasome inhibitors. *J. Immunol.* **167**, 1212–1221 (2001).
20. Herbarts, C.A. *et al.* Autoreactivity against induced or upregulated abundant self-peptides in HLA-A*0201 following measles virus infection. *Hum. Immunol.* **64**, 44–55 (2003).
21. Macdonald, W.A. *et al.* A naturally selected dimorphism within the HLA-B44 supertype alters class I structure, peptide repertoire, and T cell recognition. *J. Exp. Med.* **198**, 679–691 (2003).
22. Zhang, R., Sioma, C.S., Wang, S. & Regnier, F.E. Fractionation of isotopically labeled peptides in quantitative proteomics. *Anal. Chem.* **73**, 5142–5149 (2001).
23. Hansen, K.C. *et al.* Mass spectrometric analysis of protein mixtures at low levels using cleavable 13C-isotope-coded affinity tag and multidimensional chromatography. *Mol. Cell Proteomics* **2**, 299–314 (2003).
24. Schirle, M. *et al.* Identification of tumor-associated MHC class I ligands by a novel T cell-independent approach. *Eur. J. Immunol.* **30**, 2216–2225 (2000).
25. Falk, K., Rotzschke, O., Stevanovic, S., Jung, G. & Rammensee, H.G. Allele-specific motifs revealed by sequencing of self-peptides eluted from MHC molecules. *Nature* **351**, 290–296 (1991).
26. Seeger, F.H. *et al.* The HLA-A*6601 peptide motif: prediction by pocket structure and verification by peptide analysis. *Immunogenetics* **49**, 571–576 (1999).
27. Morris, H.R. *et al.* High sensitivity collisionally-activated decomposition tandem mass spectrometry on a novel quadrupole/orthogonal-accaleration time-of-flight mass spectrometer. *Rapid Commun. Mass Spectrom.* **10**, 889–896 (1996).